

Evaluation of mixed theories for laminated plates through the axiomatic/asymptotic method

Original

Evaluation of mixed theories for laminated plates through the axiomatic/asymptotic method / Petrolo, Marco; Cinefra, Maria; Lamberti, Alessandro; Carrera, Erasmo. - In: COMPOSITES. PART B, ENGINEERING. - ISSN 1359-8368. - STAMPA. - 76:(2015), pp. 260-272. [10.1016/j.compositesb.2015.02.027]

Availability:

This version is available at: 11583/2600362 since: 2020-04-24T14:18:03Z

Publisher:

Elsevier Ltd.

Published

DOI:10.1016/j.compositesb.2015.02.027

Terms of use:

This article is made available under terms and conditions as specified in the corresponding bibliographic description in the repository

Publisher copyright

Elsevier postprint/Author's Accepted Manuscript

© 2015. This manuscript version is made available under the CC-BY-NC-ND 4.0 license
<http://creativecommons.org/licenses/by-nc-nd/4.0/>. The final authenticated version is available online at:
<http://dx.doi.org/10.1016/j.compositesb.2015.02.027>

(Article begins on next page)

Evaluation of Mixed Theories for Laminated Plates through the Axiomatic/Asymptotic Method

M. Petrolo^{a*}; M. Cinefra^{b†}; A. Lamberti^{b‡}; E. Carrera^{b§}

^aSchool of Aerospace, Mechanical and Manufacturing Engineering, RMIT University,
PO Box 71, Bundoora VIC 3083, Australia

^bDepartment of Mechanical and Aerospace Engineering, Politecnico di Torino,
Corso Duca degli Abruzzi 24, 10129 Torino, Italy

Revised version of Ms. Ref. No.: JCOMB-D-15-00046

Author for correspondence:

E. Carrera, Professor,
Department of Mechanical and Aerospace Engineering,
Politecnico di Torino,
Corso Duca degli Abruzzi 24,
10129 Torino, Italy,
tel: +39 011 090 6836,
fax: +39 011 090 6899,
e-mail: erasmo.carrera@polito.it,
website: www.mul2.com

*Research Fellow, e-mail: marco.petrolo@rmit.edu.au

†Research Assistant, e-mail: maria.cinefra@polito.it

‡PhD Student, e-mail: alessandro.lamberti@polito.it

§Professor of Aerospace Structures and Aeroelasticity, e-mail: erasmo.carrera@polito.it

Abstract

This paper proposes variable kinematic, mixed theories for laminated plates built via the asymptotic/axiomatic method (AAM). This method has been recently developed and successfully applied to develop refined theories for multilayered plates and shells. The AAM evaluates the accuracy of each unknown variables of a structural model. The present paper extends the AAM to mixed theories based on the Reissner Mixed Variational Theorem (RMVT). The displacement transverse stress fields are modeled by means of the Carrera Unified Formulation (CUF), and expansions up to the fourth-order are employed. Equivalent Single Layer (ESL) and Layer Wise (LW) schemes are adopted, and closed-form Navier-type solutions are considered.

The AAM is exploited to determine the set of active terms of a refined plate model. The inactive terms are then discarded. The effectiveness of each variable is evaluated with respect to an LW, fourth-order mixed model. Reduced models are built for different thickness ratios, stacking sequences and displacement/stress variables.

The results suggest that reduced models with significantly less unknown variables than full models can be built with no accuracies penalties. Such models are problem dependent, and full models should be preferred in the case of thick, asymmetric plates.

Keywords: A. Laminates, Plates, C. Laminate mechanics C. Analytical modelling C. Computational modelling

1 Introduction

Laminated composite and metallic plates are commonly adopted in many engineering applications, and a number of structural models have been developed over the last decades for their analysis. The solution of the 3D elasticity equations can be very expensive from a computational standpoint, and, moreover, such solutions are usually valid only for a few geometries, material characteristics, and boundary conditions. 2D structural models are employed to analyze plates. The oldest plate model is due to Kirchhoff [1]. According to this model, transverse shear, and normal strains are assumed to be negligible with respect to the other stress and strain components. An extension of this model to multilayered structures is referred to as the Classical Lamination Theory (CLT). Further details on shell theories can be found in [2].

Refined plate models have been developed to improve the Kirchhoff model. A brief overview of some of the main techniques to develop advanced plate models for the static analysis of composite plates is presented hereinafter. In particular, the following macro categories are addressed:

- Models that account for transverse and normal shear effects.
- Layer-Wise And Zig-Zag models.
- Asymptotic approaches and the proper generalized decomposition.
- Reissner Mixed Variational Theorem (RMVT) based models.

Particular attention is paid to the latter; the main aim of this paper deals, in fact, with refined plate models based on the RMVT.

Shear effects in laminated plates can be very significant; the shear deformability in this type of plates is higher than in isotropic plates. Reissner and Mindlin [3, 4] included the shear effect, and their model is known as the First Order Shear Deformation Theory (FSDT). Further

refinements of the FSDT can be achieved through the Vlasov [5] and the Reddy-Vlasov model [6], These models account for the homogeneous conditions for the transverse shear stresses at the top and bottom plate surfaces.

Hildebrand, Reissner, and Thomas [7] developed a refined model that accounts for both the transverse shear and normal stress effects, i.e. that fulfills Koiter's recommendation [8]. Other significant contributions on laminated plate models can be found in [9, 10, 11, 12].

Multilayered structures are transversely anisotropic, and their mechanical properties are discontinuous along the thickness. These features are responsible for transverse displacements whose slopes can rapidly change at the layer interfaces and transversely discontinuous in-plane stresses. Due to equilibrium conditions, transverse stresses must be continuous at the interfaces. The Layer-Wise (LW) approach [13, 14, 15], Zig-zag models [16, 17] and mixed variational tools [18, 19, 20] have been proposed to deal with these mechanical behaviors. In the LW, each layer is seen as an independent plate and compatibility of displacement components are imposed at the interfaces. Compatibility and equilibrium conditions are then used at the interfaces to reduce the number of the unknown variables.

The plate theories mentioned above are axiomatic; the unknown variable fields are, in fact, assumed a priori, and such assumptions are based on the scientist's intuition and experience. An alternative approach is the asymptotic method in which asymptotic expansions of the unknown variables are introduced along the plate thickness. The asymptotic method provides approximate theories with known accuracy with respect to the 3D exact solution [21, 22, 23, 24]. The influence of the expansion terms is evaluated with respect to a geometrical perturbation parameter (e.g. the thickness-to-length ratio). The asymptotic approach furnishes consistent approximations; that is, all the retained terms are those which influences the solution with the same order of magnitude as the vanishing perturbation parameter.

The Proper Generalized Decomposition (PGD) decomposes a 3D problem as the summation of

a number of 1D and 2D functions [25]. PGD can be considered as a powerful tool to reduce the numerical complexity of 3D problem.

The RMVT is a mixed variational approach in which displacements and transverse stresses are the unknown variables of the structural problem. Furthermore, in an RMVT model the interlaminar continuity of transverse stresses is imposed a priori [26, 27, 28, 29]. Murakami and Toledano applied the RMVT to the analysis of multilayered plates via first and higher-order theories and layer-wise schemes [19, 30, 31].

This paper proposes refined plate models by means of the Carrera Unified Formulation (CUF)[32, 33]. According to the CUF, the displacement and stress fields of plates can be defined as arbitrary expansions of the thickness coordinate. The expansion order is a free parameter of the analysis, and it can be chosen via a convergence analysis. The governing equations are obtained through a set of fundamental nuclei whose form does not depend on either the expansion order nor the base functions. CUF models based on the RMVT have been developed over the last years [20, 34, 35, 36, 37, 38, 39, 40, 41, 42, 43].

The axiomatic/asymptotic method (AAM) has been recently developed for beams [44, 45] and plates [46, 47] in the CUF framework. The AAM investigates the effectiveness of each generalized displacement variable of a refined theory against the variation of various parameters; such as the thickness, the orthotropic ratio and the stacking sequence. The AAM leads to the definition of reduced models that have the same accuracy of the full model but that have fewer unknown variables. The best theory diagram (BTD) is an important outcome that stemmed from the use of the AAM [48]. The BTD is a diagram in which, for a given problem, the computationally cheapest structural model for a given accuracy can be read. The BTD is problem-dependent, and it can be obtained by exploiting genetic algorithms [49, 50]. The most recent developments have dealt with the definition of more accurate techniques to evaluate the accuracy of the model [51, 52], layer-wise plate [53] and shell [54] models.

In this work, the AAM is applied to RMVT models for the first time. Navier-like closed-form solutions are employed, and both ESL and LW models are considered. This paper is organized as follows: the geometrical relations for plates and the constitutive equations for laminated structures are presented in Section 2; the CUF is presented in Section 3; the governing equations are introduced in Section 4; the axiomatic/asymptotic technique and the BTM are introduced in Section 5; the results are given in Section 6; the conclusions are drawn in Section 7.

2 Geometrical and constitutive relations for plates

The plate geometry is shown in Fig. 1; the reference surface is Ω and its boundary is Γ . The reference system axes which lie on the reference surface Ω are denoted as x, y ; z is the reference axis normal to the reference surface. The length side dimensions of the plate are indicated as a and b , and the thickness of the plate is h .

The strain components for a generic k layer are evaluated according to the linear strain-displacement relation, that is

$$\boldsymbol{\epsilon}^k = \mathbf{D}\mathbf{u}^k \quad (1)$$

where \mathbf{D} is a differential operator whose components are

$$\mathbf{D} = \begin{bmatrix} \frac{\partial}{\partial x} & 0 & 0 \\ 0 & \frac{\partial}{\partial y} & 0 \\ 0 & 0 & \frac{\partial}{\partial z} \\ \frac{\partial}{\partial y} & \frac{\partial}{\partial x} & 0 \\ \frac{\partial}{\partial z} & 0 & \frac{\partial}{\partial x} \\ 0 & \frac{\partial}{\partial z} & \frac{\partial}{\partial y} \end{bmatrix} \quad (2)$$

Strain components are grouped into in-plane (p) and out-of-plane (n) components, that is

$$\boldsymbol{\epsilon}_p^k = \begin{bmatrix} \epsilon_{xx}^k & \epsilon_{yy}^k & \epsilon_{xy}^k \end{bmatrix}^T \quad \boldsymbol{\epsilon}_n^k = \begin{bmatrix} \epsilon_{xz}^k & \epsilon_{yz}^k & \epsilon_{zz}^k \end{bmatrix}^T \quad (3)$$

The superscript T denotes the transpose operation. On the basis of this grouping, it is possible to write

$$\boldsymbol{\epsilon}_p^k = \mathbf{D}_p \mathbf{u}^k \quad \boldsymbol{\epsilon}_n^k = \mathbf{D}_n \mathbf{u}^k \quad (4)$$

where

$$\mathbf{D}_p = \begin{bmatrix} \frac{\partial}{\partial x} & 0 & 0 \\ 0 & \frac{\partial}{\partial y} & 0 \\ \frac{\partial}{\partial y} & \frac{\partial}{\partial x} & 0 \end{bmatrix} \quad (5)$$

$$\mathbf{D}_n = \begin{bmatrix} \frac{\partial}{\partial z} & 0 & \frac{\partial}{\partial x} \\ 0 & \frac{\partial}{\partial z} & \frac{\partial}{\partial y} \\ 0 & 0 & \frac{\partial}{\partial z} \end{bmatrix} = \overbrace{\begin{bmatrix} 0 & 0 & \frac{\partial}{\partial x} \\ 0 & 0 & \frac{\partial}{\partial y} \\ 0 & 0 & 0 \end{bmatrix}}^{\mathbf{D}_{n\Omega}} + \overbrace{\begin{bmatrix} \frac{\partial}{\partial z} & 0 & 0 \\ 0 & \frac{\partial}{\partial z} & 0 \\ 0 & 0 & \frac{\partial}{\partial z} \end{bmatrix}}^{\mathbf{D}_{nz}} \quad (6)$$

The stress components for a generic k layer can be obtained via the constitutive equations,

$$\boldsymbol{\sigma}^k = \mathbf{C}^k \boldsymbol{\epsilon}^k \quad (7)$$

The matrix of the material elastic coefficients (\mathbf{C}) is given in the problem reference system (x, y, z). The dependence of the elastic coefficients C_{ij} on Young's modulus, Poisson's ratio, the shear modulus, and the fiber angle is not reported here. It can be found in the book by Reddy [6]. The stress components can be grouped into in-plane (p) and out-of-plane components, i.e.

$$\boldsymbol{\sigma}_p^k = \begin{bmatrix} \sigma_{xx}^k & \sigma_{yy}^k & \sigma_{xy}^k \end{bmatrix}^T \quad \boldsymbol{\sigma}_n^k = \begin{bmatrix} \sigma_{xz}^k & \sigma_{yz}^k & \sigma_{zz}^k \end{bmatrix}^T \quad (8)$$

The constitutive can be written as

$$\begin{aligned}\boldsymbol{\sigma}_p^k &= \mathbf{C}_{pp}^k \boldsymbol{\epsilon}_p^k + \mathbf{C}_{pn}^k \boldsymbol{\epsilon}_n^k \\ \boldsymbol{\sigma}_n^k &= \mathbf{C}_{np}^k \boldsymbol{\epsilon}_p^k + \mathbf{C}_{nn}^k \boldsymbol{\epsilon}_n^k\end{aligned}\tag{9}$$

In the case of orthotropic materials, the following relations hold

$$\mathbf{C}_{pp}^k = \begin{bmatrix} C_{11}^k & C_{12}^k & C_{16}^k \\ C_{12}^k & C_{22}^k & C_{26}^k \\ C_{16}^k & C_{26}^k & C_{66}^k \end{bmatrix} \quad \mathbf{C}_{nn}^k = \begin{bmatrix} C_{55}^k & C_{45}^k & 0 \\ C_{45}^k & C_{44}^k & 0 \\ 0 & 0 & C_{33}^k \end{bmatrix} \quad \mathbf{C}_{pn}^k = \mathbf{C}_{np}^{k^T} = \begin{bmatrix} 0 & 0 & C_{13}^k \\ 0 & 0 & C_{23}^k \\ 0 & 0 & C_{36}^k \end{bmatrix}\tag{10}$$

According to the RMVT, the out-of-plane stresses (σ_{xz} , σ_{yz} , and σ_{zz}) are assumed as independent, and a particular mixed form of the Hooke law is required,

$$\begin{aligned}\boldsymbol{\sigma}_{pH} &= \tilde{\mathbf{C}}_{pp}^k \boldsymbol{\epsilon}_{pG}^k + \tilde{\mathbf{C}}_{pn}^k \boldsymbol{\sigma}_{nM}^k \\ \boldsymbol{\epsilon}_{nH} &= \tilde{\mathbf{C}}_{np}^k \boldsymbol{\epsilon}_{pG}^k + \tilde{\mathbf{C}}_{nn}^k \boldsymbol{\sigma}_{nM}^k\end{aligned}\tag{11}$$

where H indicates those stress and strain components that were obtained by means of the Hooke law. G indicates those strain components that were obtained by means of the geometrical differential operators in Eqs. 5 and 6. M indicates the transverse stress components modeled by means of the CUF.

The elastic coefficient matrices are the following:

$$\tilde{\mathbf{C}}_{pp}^k = \mathbf{C}_{pp}^k - \mathbf{C}_{pn}^k \mathbf{C}_{nn}^{k^{-1}} \mathbf{C}_{np}^k \quad \tilde{\mathbf{C}}_{pn}^k = \mathbf{C}_{pn}^k \mathbf{C}_{nn}^{k^{-1}} \quad \tilde{\mathbf{C}}_{np}^k = -\mathbf{C}_{nn}^{k^{-1}} \mathbf{C}_{np}^k \quad \tilde{\mathbf{C}}_{nn}^k = \mathbf{C}_{nn}^{k^{-1}} \tag{12}$$

3 Carrera Unified Formulation for plates

In the CUF framework, the displacement field of a plate can be described as

$$\mathbf{u}(x, y, z) = F_\tau(z) \cdot \mathbf{u}_\tau(x, y) \quad \tau = 1, 2, \dots, N + 1 \quad (13)$$

where \mathbf{u} is the displacement vector $(u_x \ u_y \ u_z)$ whose components are the displacements along the x , y , and z . F_τ are the expansion functions and $\mathbf{u}_\tau = (u_{x\tau}, u_{y\tau}, u_{z\tau})$ are the displacement variables of a point P_Ω which lies on the reference surface Ω ; N is the expansion order. For the sake of clarity, Eq. 13 is also given as follows:

$$\begin{aligned} u_x &= F_1 u_{x1} + F_2 u_{x2} + \dots + F_N u_{xN} + F_{N+1} u_{xN+1} \\ u_y &= F_1 u_{y1} + F_2 u_{y2} + \dots + F_N u_{yN} + F_{N+1} u_{yN+1} \\ u_z &= F_1 u_{z1} + F_2 u_{z2} + \dots + F_N u_{zN} + F_{N+1} u_{zN+1} \end{aligned} \quad (14)$$

A number of explicit displacement fields will be given for specific expansion orders in the following sections of this paper. According to the RMVT, the transverse stress components (σ_{xz} , σ_{yz} and σ_{zz}) are modeled as

$$\boldsymbol{\sigma}_{nM}(z, y, z) = \begin{bmatrix} \sigma_{xzM}(x, y, z) \\ \sigma_{yzM}(x, y, z) \\ \sigma_{zzM}(x, y, z) \end{bmatrix} = F_\tau(z) \begin{bmatrix} \sigma_{xzM\tau}(x, y) \\ \sigma_{yzM\tau}(x, y) \\ \sigma_{zzM\tau}(x, y) \end{bmatrix} \quad \tau = 1, 2, \dots, N + 1 \quad (15)$$

That is,

$$\begin{aligned} \sigma_{xzM} &= F_1 \sigma_{xzM_1} + F_2 \sigma_{xzM_2} + \dots + F_N \sigma_{xzM_N} + F_{N+1} \sigma_{xzM_{N+1}} \\ \sigma_{yzM} &= F_1 \sigma_{yzM_1} + F_2 \sigma_{yzM_2} + \dots + F_N \sigma_{yzM_N} + F_{N+1} \sigma_{yzM_{N+1}} \\ \sigma_{zzM} &= F_1 \sigma_{zzM_1} + F_2 \sigma_{zzM_2} + \dots + F_N \sigma_{zzM_N} + F_{N+1} \sigma_{zzM_{N+1}} \end{aligned} \quad (16)$$

The expansion functions F_τ can be defined along the entire thickness of the plate or each layer. In the former case, the Equivalent Single Layer (ESL) approach is followed and in the latter case the Layer Wise (LW) method is used. Examples of ESL and LW schemes are shown in Figs 2(a) and 2(b), respectively; a transverse section of a multilayered plate is shown, and the number of layers is equal to N_L . A generic displacement component distribution is presented according to linear and higher-order expansions.

3.1 Equivalent Single Layer models

According to the ESL, the behavior of a multilayered plate is analyzed considering it as a single equivalent lamina. F_τ can be Mac-Laurin expansions of z , and they are defined as $F_\tau = z^{\tau-1}$. CUF ESL models based on the Principle of Virtual Displacements (PVD) are referred to as EDN, where N is the expansion order. CUF RMVT ESL models are referred to as EMN. In the latter case, the transversal stresses are always modeled by means of the LW scheme with an expansion order equal to N . An example of a fourth-order (ED4) displacement field is the following:

$$\begin{aligned} u_x &= u_{x_1} + z u_{x_2} + z^2 u_{x_3} + z^3 u_{x_4} + z^4 u_{x_5} \\ u_y &= u_{y_1} + z u_{y_2} + z^2 u_{y_3} + z^3 u_{y_4} + z^4 u_{y_5} \\ u_z &= u_{z_1} + z u_{z_2} + z^2 u_{z_3} + z^3 u_{z_4} + z^4 u_{z_5} \end{aligned} \quad (17)$$

3.2 Layer Wise models

In an LW model, the displacement field is C_0 continuous through the laminate thickness. LW models can be conveniently built by using the Legendre polynomial expansion along each layer. The displacement field is described as

$$\mathbf{u}^k = F_t \cdot \mathbf{u}_t^k + F_b \cdot \mathbf{u}_b^k + F_r \cdot \mathbf{u}_r^k = F_\tau \mathbf{u}_\tau^k \quad \tau = t, b, r \quad r = 2, 3, \dots, N \quad k = 1, 2, \dots, N_l \quad (18)$$

Subscripts t , and b indicate the top and the bottom of the layer. An example of LD4 displacement field is the following:

$$\begin{aligned} u_x^k &= F_t u_{xt}^k + F_2 u_{x2}^k + F_3 u_{x3}^k + F_4 u_{x4}^k + F_b u_{xb}^k \\ u_y^k &= F_t u_{yt}^k + F_2 u_{y2}^k + F_3 u_{y3}^k + F_4 u_{y4}^k + F_b u_{yb}^k \\ u_z^k &= F_t u_{zt}^k + F_2 u_{z2}^k + F_3 u_{z3}^k + F_4 u_{z4}^k + F_b u_{zb}^k \end{aligned} \quad (19)$$

The LW can be employed to define the transverse stress components,

$$\boldsymbol{\sigma}_n^k = F_t \boldsymbol{\sigma}_{nt}^k + F_r \boldsymbol{\sigma}_{nr}^k + F_b \boldsymbol{\sigma}_{nb}^k \quad \tau = t, b, r \quad r = 2, 3, \dots, N \quad k = 1, 2, \dots, N_l \quad (20)$$

F_τ are defined via an non-dimensional coordinate (ζ_k , its range is $-1 \leq \zeta_k \leq 1$). The extremal values -1 and 1 denote the bottom and the top of the layer, respectively. F_τ are given by the Legendre polynomials,

$$F_t = \frac{P_0 + P_1}{2} \quad F_b = \frac{P_0 - P_1}{2} \quad F_r = P_r - P_{r-2} \quad r = 2, 3, \dots, N \quad (21)$$

The fourth-order Legendre polynomials are

$$P_0 = 1 \quad P_1 = \zeta_k \quad P_2 = \frac{3\zeta_k^2 - 1}{2} \quad P_3 = \frac{5\zeta_k^3 - 3\zeta_k}{2} \quad P_4 = \frac{35\zeta_k^4}{8} - \frac{15\zeta_k^2}{4} + \frac{3}{8} \quad (22)$$

CUF LW PVD models are referred to as LDN, where N is the expansion order. In the RMVT case, models are referred to as LMN.

4 Governing equations

The PVD stats that

$$\sum_{k=1}^{N_L} \delta L_{int}^k = \sum_{k=1}^{N_L} \delta L_{ext}^k \quad (23)$$

Where δL_{int}^k is the virtual variation of the strain energy given by the stress and strain distributions in a generic layer k . δL_{ext} is the virtual variation of the work made by the external loadings. The PVD can be expressed as

$$\sum_{k=1}^{N_L} \int_{\Omega_k} \int_{A_k} (\delta \epsilon_p^T \sigma_p + \delta \epsilon_n^T \sigma_n) dA_k d\Omega_k = \sum_{k=1}^{N_L} \int_{\Omega_k} \int_{A_k} \delta \mathbf{u}^T \mathbf{p} dA_k d\Omega_k \quad (24)$$

where Ω_k stands for the reference surface of the layer, and $\int_{A_k} dA_k$ denotes the integration along the thickness direction.

In the RMVT case, the compatibility of the transverse strains is enforced in addition to the equilibrium,

$$\sum_{k=1}^{N_L} \int_{\Omega_k} \int_{A_k} [\delta \epsilon_{pG}^T \sigma_{pH} + \delta \epsilon_{nG}^T \sigma_{nM} + \delta \sigma_{nM}^T (\epsilon_{nG} - \epsilon_{nH})] dA_k d\Omega_k = \sum_{k=1}^{N_L} \int_{\Omega_k} \int_{A_k} \delta \mathbf{u}^T \mathbf{p} dA_k d\Omega_k \quad (25)$$

The mixed term $\delta \sigma_{nM}^T (\epsilon_{nG} - \epsilon_{nH})$ enforces the compatibility of the transverse strain components ϵ_n . In the following, the subscript G indicates the strains obtained by means of the differential operators defined in Eq.s 5 and 6, and the subscript H indicates the stresses obtained by means of the Hooke law.

4.1 PVD case

According to the CUF displacement field, the geometrical and constitutive equations, the PVD can be written as

$$\begin{aligned}
& \int_{\Omega_k} \delta \mathbf{u}_s^k \left\{ (-\mathbf{D}_p)^T \left[\mathbf{C}_{pp}^k E_{s\tau} \mathbf{D}_p + \mathbf{C}_{pn}^k E_{s\tau} \mathbf{D}_{n\Omega} + \mathbf{C}_{pn}^k E_{s\tau,z} \right] \right. \\
& \quad + (-\mathbf{D}_{n\Omega})^T \left[\mathbf{C}_{pn}^{kT} E_{s\tau} \mathbf{D}_p + \mathbf{C}_{nn}^k E_{s\tau} \mathbf{D}_{n\Omega} + \mathbf{C}_{nn}^k E_{s\tau,z} \right] \\
& \quad \left. + \left[\mathbf{C}_{pn}^{kT} E_{s,z\tau} \mathbf{D}_p + \mathbf{C}_{nn}^k E_{s,z\tau} \mathbf{D}_{n\Omega} + \mathbf{C}_{nn}^k E_{s,z\tau,z} \right] \right\} \mathbf{u}_\tau^k d\Omega_k + \\
& \int_{\Gamma_k} \delta \mathbf{u}_s^k \left\{ (\mathbf{I}_p)^T \left[\mathbf{C}_{pp}^k E_{s\tau} \mathbf{D}_p + \mathbf{C}_{pn}^k E_{s\tau} \mathbf{D}_{n\Omega} + \mathbf{C}_{pn}^k E_{s\tau,z} \right] \right. \\
& \quad \left. + (\mathbf{I}_{n\Omega})^T \left[\mathbf{C}_{pn}^{kT} E_{s\tau} \mathbf{D}_p + \mathbf{C}_{nn}^k E_{s\tau} \mathbf{D}_{n\Omega} + \mathbf{C}_{nn}^k E_{s\tau,z} \right] \right\} \mathbf{u}_\tau^k d\Gamma_k = \delta L_e^k
\end{aligned} \tag{26}$$

Where \mathbf{I}_p and \mathbf{I}_{np} are

$$\mathbf{I}_p = \begin{bmatrix} 1 & 0 & 0 \\ 0 & 1 & 0 \\ 1 & 1 & 0 \end{bmatrix} \quad \mathbf{I}_{np} = \begin{bmatrix} 0 & 0 & 1 \\ 0 & 0 & 1 \\ 0 & 0 & 0 \end{bmatrix} \tag{27}$$

$(E_{\tau s}, E_{\tau,zs}, E_{\tau s,z}, E_{\tau,zs,z})$ are defined as

$$(E_{\tau s}, E_{\tau,zs}, E_{\tau s,z}, E_{\tau,zs,z}) = \int_{-\frac{h_k}{2}}^{\frac{h_k}{2}} (F_\tau F_s, F_{\tau,z} F_s, F_\tau F_{s,z}, F_{\tau,z} F_{s,z},) dz_k \tag{28}$$

Where h_k is thickness of the generic k layer. The governing equations can be written as

$$\delta \mathbf{u}_s^{kT} : \mathbf{K}_d^{\tau s} \cdot \mathbf{u}_\tau^k = \mathbf{P}_{u\tau}^\tau \tag{29}$$

and the boundary conditions are

$$\mathbf{\Pi}_d^{k\tau s} \mathbf{u}_\tau^k = \mathbf{\Pi}_d^{k\tau s} \bar{\mathbf{u}}_\tau^k \tag{30}$$

Where $\mathbf{P}_{d\tau}^\tau$ is the external load. The fundamental nucleus $\mathbf{K}_d^{\tau s}$ is assembled through the indexes τ and s . The fundamental nucleus is

$$\begin{aligned} \mathbf{K}_d^{\tau s} = & \left\{ (-\mathbf{D}_p)^T \left[\mathbf{C}_{pp}^k E_{s\tau} \mathbf{D}_p + \mathbf{C}_{pn}^k E_{s\tau} \mathbf{D}_{n\Omega} + \mathbf{C}_{pn}^k E_{s\tau,z} \right] + \right. \\ & (-\mathbf{D}_{n\Omega})^T \left[\mathbf{C}_{pn}^{kT} E_{s\tau} \mathbf{D}_p + \mathbf{C}_{nn}^k E_{s\tau} \mathbf{D}_{n\Omega} + \mathbf{C}_{nn}^k E_{s\tau,z} \right] + \\ & \left. + \left[\mathbf{C}_{pn}^{kT} E_{s,z\tau} \mathbf{D}_p + \mathbf{C}_{nn}^k E_{s,z\tau} \mathbf{D}_{n\Omega} + \mathbf{C}_{nn}^k E_{s,z\tau,z} \right] \right\} \end{aligned} \quad (31)$$

And for boundary conditions,

$$\begin{aligned} \mathbf{\Pi}_d^{k\tau s} = & \left\{ (\mathbf{I}_p)^T \left[\mathbf{C}_{pp}^k E_{s\tau} \mathbf{D}_p + \mathbf{C}_{pn}^k E_{s\tau} \mathbf{D}_{n\Omega} + \mathbf{C}_{pn}^k E_{s\tau,z} \right] + \right. \\ & \left. + (\mathbf{I}_{n\Omega})^T \left[\mathbf{C}_{pn}^{kT} E_{s\tau} \mathbf{D}_p + \mathbf{C}_{nn}^k E_{s\tau} \mathbf{D}_{n\Omega} + \mathbf{C}_{nn}^k E_{s\tau,z} \right] \right\} \end{aligned} \quad (32)$$

4.2 RMVT case

According to the RMVT,

$$\begin{aligned} & \sum_{k=1}^{N_L} \int_{\Gamma_k} \delta \mathbf{u}_s^{kT} \left\{ \mathbf{I}_p^T \tilde{\mathbf{C}}_{pp}^k E_{\tau s} \mathbf{D}_p \mathbf{u}_\tau^k + \mathbf{I}_p^T \tilde{\mathbf{C}}_{pn}^k E_{\tau s} \boldsymbol{\sigma}_{n\tau}^k + \mathbf{I}_{n\Omega}^T E_{\tau s} \boldsymbol{\sigma}_{n\tau} \right\} d\Gamma_k - \\ & \sum_{k=1}^{N_L} \int_{\Omega_k} \left\{ \delta \mathbf{u}_s^{kT} \left[\mathbf{D}_p^T \tilde{\mathbf{C}}_{pp}^k E_{\tau s} \left(\mathbf{D}_p \mathbf{u}_\tau^k \right) + \mathbf{D}_p^T \tilde{\mathbf{C}}_{pn}^k E_{\tau s} \boldsymbol{\sigma}_{n\tau}^k + \mathbf{D}_{n\Omega}^T E_{\tau s} \boldsymbol{\sigma}_{n\tau} + E_{\tau s,z} \boldsymbol{\sigma}_{n\tau} \right] + \right. \\ & \quad \left. + \delta \boldsymbol{\sigma}_{ns}^T \left[\mathbf{D}_{n\Omega} E_{\tau s} \mathbf{u}_\tau^k + E_{\tau,z} \mathbf{u}_\tau^k - \tilde{\mathbf{C}}_{np}^k E_{\tau s} \left(\mathbf{D}_p \mathbf{u}_\tau^k \right)^k - \tilde{\mathbf{C}}_{nn}^k E_{\tau s} \boldsymbol{\sigma}_{n\tau}^k \right] \right\} d\Omega_k = \\ & \sum_{k=1}^{N_L} \int_{\Omega_k} \int_{A_k} \delta (F_s \mathbf{u}_s)^T \mathbf{p} dA_k d\Omega_k \end{aligned} \quad (33)$$

The equilibrium equations can be written as

$$\begin{aligned} \mathbf{K}_{uu}^{k\tau s} \mathbf{u}_\tau^k + \mathbf{K}_{u\sigma}^{k\tau s} \boldsymbol{\sigma}_\tau^k &= \mathbf{p}^k \\ \mathbf{K}_{\sigma u}^{k\tau s} \mathbf{u}_\tau^k + \mathbf{K}_{\sigma\sigma}^{k\tau s} \boldsymbol{\sigma}_\tau^k &= 0 \end{aligned} \quad (34)$$

Whereas the boundary conditions are

$$\mathbf{\Pi}_u^{k\tau s} \mathbf{u}_\tau^k + \mathbf{\Pi}_\sigma^{k\tau s} \boldsymbol{\sigma}_{n\tau}^k = \mathbf{\Pi}_u^{k\tau s} \bar{\mathbf{u}}_\tau^k + \mathbf{\Pi}_\sigma^{k\tau s} \bar{\boldsymbol{\sigma}}_{n\tau}^k \quad (35)$$

The introduced differential arrays are given by the following relations:

$$\begin{aligned} \mathbf{K}_{uu}^{k\tau s} &= -\mathbf{D}_p^T \tilde{\mathbf{C}}_{pp}^k \mathbf{D}_p E_{\tau s} \\ \mathbf{K}_{u\sigma}^{k\tau s} &= -\mathbf{D}_p^T \tilde{\mathbf{C}}_{pn}^k E_{\tau s} + \mathbf{I} E_{\tau s, z} - \mathbf{D}_{n\Omega}^T E_{\tau s} \\ \mathbf{K}_{\sigma u}^{k\tau s} &= \mathbf{D}_{n\Omega} E_{\tau s} + \mathbf{I} E_{\tau, z, s} - \tilde{\mathbf{C}}_{np}^k \mathbf{D}_p E_{\tau s} \\ \mathbf{K}_{\sigma\sigma}^{k\tau s} &= -\tilde{\mathbf{C}}_{nn}^k E_{\tau s} \\ \mathbf{\Pi}_u^{k\tau s} &= \mathbf{I}_p^T \tilde{\mathbf{C}}_{pp}^k \mathbf{D}_p E_{\tau s} \\ \mathbf{\Pi}_\sigma^{k\tau s} &= \mathbf{I}_p^T \tilde{\mathbf{C}}_{pn}^k E_{\tau s} + \mathbf{I}_{n\Omega}^T E_{\tau s} \end{aligned} \quad (36)$$

\mathbf{I} is

$$\mathbf{I} = \begin{bmatrix} 1 & 0 & 0 \\ 0 & 1 & 0 \\ 0 & 0 & 1 \end{bmatrix} \quad (37)$$

4.3 Navier-type closed-form solution

This paper exploited closed-form solutions for simply-supported, cross-ply, rectangular plates under a transverse distribution of harmonic loadings. The following properties hold

$$\tilde{C}_{pp16} = \tilde{C}_{pp26} = \tilde{C}_{pn36} = \tilde{C}_{nn45} = 0 \quad (38)$$

Stresses and displacements are expressed according to the following harmonic form:

$$\begin{aligned}
(u_{x_\tau}^k \ \sigma_{xz\tau}^k) &= \left(\hat{U}_{x_\tau}^k \ \hat{\sigma}_{xz\tau}^k \right) \cos \left(\frac{m\pi x_k}{a_k} \right) \sin \left(\frac{n\pi y_k}{b_k} \right) & k = 1, N_l \\
(u_{y_\tau}^k \ \sigma_{yz\tau}^k) &= \left(\hat{U}_{y_\tau}^k \ \hat{\sigma}_{yz\tau}^k \right) \sin \left(\frac{m\pi x_k}{a_k} \right) \cos \left(\frac{n\pi y_k}{b_k} \right) & \tau = 1, N \\
(u_{z_\tau}^k \ \sigma_{zz\tau}^k) &= \left(\hat{U}_{z_\tau}^k \ \hat{\sigma}_{zz\tau}^k \right) \sin \left(\frac{m\pi x_k}{a_k} \right) \sin \left(\frac{n\pi y_k}{b_k} \right)
\end{aligned} \tag{39}$$

where $\hat{U}_{x_\tau}^k, \hat{U}_{y_\tau}^k, \hat{U}_{z_\tau}^k, \hat{\sigma}_{xz\tau}^k, \hat{\sigma}_{yz\tau}^k$ and $\hat{\sigma}_{zz\tau}^k$ are the amplitudes, m and n are the number of waves (they range from 0 to ∞) and a_k and b_k are the dimensions of the plate.

5 The axiomatic/asymptotic method

The AAM is a technique that allows us to determine the influence of each unknown variable on the solution. Axiomatically built models are used as starting theories, and their variables are investigated. As in an asymptotic analysis, the influence of each variable can be easily investigated against various parameters, e.g. thickness, orthotropic ratio, and stacking sequence. One of the main capabilities of the AAM is the definition of reduced models in which all the ineffective terms are discarded. AAM examples can be found in [46] for plates, in [44] for beams, or in [51] for shells.

The AAM consists of the following steps:

1. Parameters such as the geometry, BCs, materials and layer layouts are fixed.
2. A set of output parameters is chosen, such as displacement or stress components.
3. A starting theory is fixed (axiomatic part); that is, the displacement variables to be analyzed are defined; usually, a theory which provides 3D-like solutions is chosen; a reference solution is defined (in the present work the LM4 was adopted, since this fourth-order model offers an excellent agreement with the three-dimensional solutions as highlighted in [29]).

4. The CUF is used to generate the governing equations for the theories considered.
5. The effectiveness of each term of the adopted expansion is evaluated by evaluating the error due to its deactivation; a term is considered as non-effective if the error is negligible; the deactivation of a term is obtained by means of a penalty technique.
6. The most suitable structural model for a given structural problem is then obtained by discarding all the non-effective variables.

The penalty technique requires the use of a penalty value on the main diagonal term of the stiffness matrix related to the degrees of freedom to be deactivated. More details about the penalty technique can be found in [55], and a detailed description on the application of the penalty technique in CUF models can be found in [56].

A graphical notation was introduced to show the results. In the case of mixed formulations, a table with six lines is used, and a number of columns equal to the number of the unknown variables employed in the expansion. Table 1 shows LM4 and EM4 models for a two-layer plate. Each unknown variable can be deactivated as shown in Table 2. The symbol ■ is used to denote the terms that cannot be deactivated in the LW since this would introduce an extra constraint. Table 3 shows a reduced LM4 model in which the top-layer u_{x3} , u_{z4} , and the bottom-layer σ_{yz2} and σ_{zz4} were deactivated.

The error due to the deactivation of a displacement or stress variable is computed as

$$err = \left\| 1 - \frac{Q}{Q_{ref}} \right\| \times 100 \quad (40)$$

where Q is the displacement/stress value obtained by means of the reduced model and Q_{ref} is the reference value.

6 Results

The results of the AAM analyzes are reported hereafter; the aim is to evaluate reduced models that are based on mixed and displacement formulations. In all cases, the acting load is a transverse pressure applied to the top surface of the plate,

$$p_z = p_z^0 \sin\left(\frac{m\pi}{a}x\right) \sin\left(\frac{n\pi}{b}y\right) \quad (41)$$

where $m = n = 1$. The reference system layout is depicted in Fig. 1. In all the following analyzes, displacement and stress component values are presented in a non-dimensional form,

$$\bar{u}_z = \frac{100 u_z E_T h^3}{p_0 a^4} \quad \bar{\sigma}_{xx} = \frac{\sigma_{xx}}{p_0 (a/h)^2} \quad \bar{\sigma}_{xz\{yz\}} = \frac{\sigma_{xz\{yz\}}}{p_0 a/h} \quad (42)$$

6.1 Laminated plates

A reference solution must be available to carry out an AAM analysis. If exact 3D elasticity solutions are not available, the CUF higher-order models are used as reference solutions. These models, in fact, were proven to be as accurate as exact 3D solutions [29]. In particular, LM4 models are extremely accurate in the laminated plate analysis.

A preliminary assessment was carried out to highlight LM4 enhanced capabilities against exact 3D elasticity solutions [57]. The material properties are $E_L/E_T = 25$, $\nu = 0.25$, $G_{LT}/E_T = G_{TT}/E_T = 0.5$, $G_{Lz}/E_T = 0.2$, $0^\circ/90^\circ/0^\circ$. Table 4 shows stress and displacement values for a thin and a thick plate; the LM4 results are in excellent agreement with the exact solution. On the basis of this outcome, the AAM reference solution is the LM4 for all this paper assessments. Reduced ED4 and EM4 models are shown in Table 5 for σ_{xx} . Thin and thick plates were considered. M_e/M indicates the ratio between the number of effective terms and the number of variables of the full model. In the case of thin plates, the reduced ED4 model that is able to

provide the same accuracy as an LM4 model in the computation of σ_{xx} is the following:

$$\begin{aligned} u_x &= z u_{x_2} + z^3 u_{x_4} \\ u_y &= z u_{y_2} \\ u_z &= u_{z_1} + z^2 u_{z_3} \end{aligned} \tag{43}$$

Figure 3 shows the stress distribution given by the reduced models. A perfect match with the reference LM4 model was found. In the case of thick plates, all the variables are needed and the error is not negligible. In other words, ESL models are not able to provide the same accuracy of an LM4 model for the computation of σ_{xx} in thick plates.

Reduced LD4 and LM4 models are reported in Tables 6 and 7, respectively. Various displacement and stress components were considered for thin and thick plates. The last row refers to those reduced models that are needed to detect all the considered displacement and stress components. Figure 4 shows the shear stress distribution along the thickness of the plate; the reduced models were compared with the full LM4 model.

An asymmetric stacking sequence was then considered ($0^\circ/90^\circ$). The LM4 reference values for the AAM are reported in Table 8 together with the results from LD4, ED4, and EM4.

Table 9 shows reduced EM4 and ED4 models for u_z . In the case of thin plates, the reduced ED4 model that is able to provide the same accuracy as an LM4 model in the computation of u_z is the following:

$$\begin{aligned} u_x &= u_{x_1} + z u_{x_2} \\ u_y &= u_{y_1} + z u_{y_2} \\ u_z &= u_{z_1} + z^2 u_{z_3} \end{aligned} \tag{44}$$

All the variables are needed in the thick plate case and the error is not negligible.

Reduced LD4 and LM4 models are reported in Tables 10 and 11, respectively. The axial (σ_{xx}) and shear (σ_{yz}) stress distributions along the thickness are shown in Figs 5 and 6; the reduced

LD4 and LM4 models were considered together with the full LM4 model.

On the basis of these results, it can be stated that

- As expected, thin plates require less unknown variables to obtain the same accuracy of the full model. The AAM can lead to reduced models that require about half of the unknown variables of the full model.
- ESL reduced models with significantly fewer variables than full models can be found in the thin plate case. On the other hand, Full ESL models are needed for the thick case.
- The adoption of mixed models makes the set of active displacement variables changes with respect to the displacement model case. In other words, the introduction of stress variables makes some displacement variables ineffective and others effective.
- The LM4 reduced models are more cumbersome than the LD4 reduced models. LM4 models are however more effective in detecting the stress distributions along the thickness than LD4 reduced models. The latter sometimes are not very accurate at the top and bottom regions and do not guarantee the transverse stress interlaminar continuity. It must be underlined that LD4 reduced models that can fulfill the top and bottom BCs can be obtained by means of other AAM strategies as shown in [53].
- The asymmetry of the lamination and the increase of the thickness make the number of active terms increase. In fact, as soon as multiple displacements and stress components are needed, full models are generally preferable in the thick plate case. Reduced models with considerable fewer degrees of freedom are available for the thin plate case, or for thick plates with symmetric lamination.

6.2 Bimetallic plate

A bimetallic square plate was considered as second study case. The top layer of the plate is made of titanium ($E = 114$ GPa, $\nu = 0.3$) and the bottom layer is aluminum ($E = 70.3$ GPa, $\nu = 0.33$). The reference LM4 results employed in the axiomatic/asymptotic analysis are reported in Table 12 together with the results from LD4, ED4, and EM4.

Table 13 shows the ED4 and EM4 models for u_z . Similarly to the composite laminated plate case, thin plates can be analysed by means of reduced models. Thick plates, instead, require full models and their accuracy is poorer than LM4. In the case of thin plates, the reduced ED4 model that is able to provide the same accuracy as an LM4 model in the computation of u_z is the following:

$$\begin{aligned} u_x &= u_{x_1} + z u_{x_2} \\ u_y &= u_{y_1} + z u_{y_2} \\ u_z &= u_{z_1} + z u_{y_2} + z^2 u_{z_3} \end{aligned} \tag{45}$$

Tables 14 and 15 present the reduced LD4 and LM4 models, respectively. Figure 7 shows the shear stress distribution by means of the reduced models.

The results suggest the following:

- As for the laminated case, the increase of the thickness makes the number of active terms increase.
- A significant computational cost reduction can be obtained by means of ESL model for the thin plate case. As for the laminated case, full ESL models should be used for thick plates.
- It is hard to predict the reduced LM4 model on the basis of the LD4 one. In fact, as it he previous case, mixed reduced models may not share all the displacement variables with the LD4 model.

- It is confirmed that the LM4 reduced models are generally more cumbersome than the LD4 reduced models. The LM4 models are effective in detecting the stress distributions along the thickness. The LD4 reduced models may not fulfill the top/bottom boundary conditions as well as the interlaminar continuity of the shear stress.
- As a general guideline, as soon as multiple displacement and stress components are needed, full models should be generally preferred in the thick plate case.

7 Conclusion

The axiomatic/asymptotic method AAM has been applied for the first time to refined plate models based on the Carrera Unified Formulation (CUF) and the Reissner Mixed Variational Theorem (RMVT). The CUF leads to the generation of any order structural model with no need for formal changes in the governing equations. Such equations have been formulated via the RMVT to deal with plate models in which the displacement components and the transverse stress components are the primary variables. The AAM is a technique that can be exploited to evaluate the influence of each displacement/stress variable in a structural theory. In particular, the AAM allows us to discard all those variables that are not effective. The AAM leads to the definition of reduced structural models that are as accurate the full models, but computationally less cumbersome.

Navier closed-form solutions have been adopted in this paper. Laminated composite and bimetallic plates have been considered. The influence of different parameters, namely the thickness and the stacking sequence, has been investigated.

The following main conclusions and guidelines can be drawn:

1. The AAM can build reduced models that have considerably less unknown variables than the full models. In many cases, less than half of the original variables are required.

2. As expected, an asymmetric lamination or a thick plate, require more cumbersome models.
3. ESL reduced models can be built for thin plates, and a significant computational cost reduction can be pursued. Full ESL models should be used in the thick plate case.
4. Mixed reduced models (LM4) are more cumbersome than the models based on the displacement formulation (LD4) . However, the LM4 fulfill the top/bottom boundary conditions and the interlaminar continuity, whereas, in some cases, the LD4 do not.
5. Different output variables can require different reduced models.
6. In general, it is not possible to predict the effectiveness of the reduced LM4 on the basis of the reduced LD4; LM4 may not share all the displacement variables with the LD4 model.
7. If thick asymmetric plates have to be dealt with, and various output variable are of interest, full models have to be used.

As seen in previous works, the AAM results are problem dependent. Depending on the problem characteristics, AAM can lead to significant reductions of the number of variables, or can just recommend the use of full models. In LW models, in particular, the reduction of variables is always significant. It is also confirmed that the ease of implementation of AAM in the CUF framework allows us to:

1. Outline guidelines and recommendations for the choice of the most appropriate set of variables for any combinations of structural configurations.
2. Evaluate the accuracy of any given structural theory for different structural configurations against exact or quasi-exact solutions.

Future works will deal with the construction of best theory diagrams (BTDs) for RMVT models via genetic algorithms. As shown in [49, 50, 54], the combined use of AAM, CUF and genetic

algorithms lead to the definition of a BTM in which, for a given accuracy, the least cumbersome structural model can be read. The use of the genetic algorithm reduces considerably the number of reduced models to be considered to build the BTM.

References

- [1] Kirchhoff, G. "Über das Gleichgewicht und die Bewegung einer elastischen Scheibe" *Journal für reine und angewandte Mathematik*, 40:51–88, 1850. doi: 10.1515/crll.1850.40.51.
- [2] Kraus, H. *Thin Elastic Shells*. John Wiley & Sons, 1967.
- [3] Reissner, E. The effect of transverse shear deformation on the bending of elastic plates. *Journal of Applied Mechanics*, 12:69–76, 1945.
- [4] Mindlin, R.D. Influence of rotatory inertia and shear in flexural motions of isotropic elastic plates. *Journal of Applied Mechanics*, 18:1031–1036, 1951.
- [5] Vlasov, B.F. On the equations of Bending of plates. *Dokl. Ak. Nauk. Azerbejanskoi-SSR*, 3:955–979, 1957.
- [6] Reddy, J. N. *Mechanics of Laminated Plates, Theory and Analysis*. CRC Press, Boca Raton, 1997.
- [7] Hildebrand, F.B. and Reissner, E. and Thomas G.B. Notes in the foundations of the theory of small displacement of orthotropic shells. Technical report, NASA, March.
- [8] Koiter, W.T. A consistent first approximation in the general theory of thin elastic shells. In *Proc. of Symp. on the Theory of Thin Elastic Shells*, Noth-Holland, Amsterdam, August 1959.

- [9] Librescu, L. and Reddy, J.N. “A critical review and generalization of transverse shear deformable anisotropic plates, euromech colloquium 219, kassel”, *Refined Dynamical Theories of Beams, Plates and Shells and Their Applications*, September 1986, pp. 32–43, I Elishakoff and Irretier (eds), Springer Verlag, Berlin.
- [10] Noor, A. K. and Burton, W. S. “Assessment of shear deformation theories for multilayered composite plates”, *Appl. Mech. Rev.*, Vol. 42, No. 1, 1989, pp. 1–18.
- [11] Kapania, K. and Raciti, S. “Recent advances in analysis of laminated beams and plates, part I: Shear effects and buckling”, *AIAA Journal*, Vol. 27, No. 7, 1989, pp. 923–935.
- [12] Reddy, J. N. and Robbins, D. H. “Theories and computational models for composite laminates”, *Appl. Mech. Rev.*, Vol. 47, No. 6, 1994, pp. 147–165.
- [13] Srinivas, S. A refined analysis of composite laminates. *Journal of Sound and Vibration*, 30:495–507, 1973.
- [14] Cho, K.N. and Bert, C.W. and Striz, A.G. Free Vibrations of Laminated Rectangular Plates Analyzed by Higher order Individual-Layer Theory. *Journal of Sound and Vibration*, 145:429–442, 1991.
- [15] Robbins Jr, D.H. and Reddy, J.N. Modeling of thick composites using a layer-wise theory. *International Journal for Numerical Methods in Engineering*, 36:655–677, 1993.
- [16] Lekhnitskii, S.G. Strength Calculation of Composite Beams. *Vestnik Inzhen. i Tekhnikov*, 9, 1935.
- [17] Ambartsumian, S. A. On a theory of bending of anisotropic plates. *Investiia Akad. Nauk SSSR*, 4, 1958.

- [18] Reissner, E. On a certain mixed variational theory and a proposed application. *International Journal for Numerical Methods in Engineering*, 20:1366-1368, 1984.
- [19] Murakami, H. Laminated composite plate theory with improved in-plane responses. *Journal of Applied Mechanics*, 53:661-666, 1986.
- [20] Carrera, E. Mixed layer-wise models for multilayered plates analysis. *Composite Structures*, 43(1):57–70, 1998. [http://dx.doi.org/10.1016/S0263-8223\(98\)00097-X](http://dx.doi.org/10.1016/S0263-8223(98)00097-X).
- [21] Cicala, P. “Sulla teoria elastica della parete sottile”, *Giornale del Genio Civile*, Vol. 4, 6 and 9, 1959.
- [22] Yu, W. and Hodges, D.H. and Volovoi, V.V. Asymptotically accurate 3-D recovery from Reissner-like composite plate finite elements. *Computers and Structures*, 81(7):439–454, 2003. [http://dx.doi.org/10.1016/S0045-7949\(03\)00011-7](http://dx.doi.org/10.1016/S0045-7949(03)00011-7).
- [23] Berdichevsky, V.L. An asymptotic theory of sandwich plates. *International Journal of Engineering Science*, 48(3):383–404, 2010. <http://dx.doi.org/10.1016/j.ijengsci.2009.09.001>.
- [24] Lee, C.Y. and Yu, W. Homogenization and dimensional reduction of composite plates with in-plane heterogeneity. *International Journal of Solids and Structures*, 48(10):1474–1484, 2011. <http://dx.doi.org/10.1016/j.ijsolstr.2011.01.032>.
- [25] Bognet, B. and Bordeu, F. and Chinesta, F. and Leygue, A. and Poitou, A. Advanced simulation of models defined in plate geometries: 3D solutions with 2D computational complexity. *Computer Methods in Applied Mechanics and Engineering*, 201–204:1–12, 2012. <http://dx.doi.org/10.1016/j.cma.2011.08.025>.
- [26] Reissner, E. On a certain mixed variational theory and a proposed application *International Journal for Numerical Methods in Engineering* , 20:1366–1368, 1984.

- [27] Reissner, E. Reflections on the theory of elastic plates *Applied Mechanics Review* , 38:1453–1464, 1985.
- [28] Reissner, E. On a mixed variational theorem and on a shear deformable plate theory *International Journal for Numerical Methods in Engineering* , 23:193–198, 1986.
- [29] Carrera, E. Developments, ideas, and evaluations based upon Reissner’s Mixed Variational Theorem in the modeling of multilayered plates and shells *Applied Mechanics Reviews* , 54(4):301–329, 2001.
- [30] Toledano, A. and Murakami, H. A high-order laminated plate theory with improved in-plane responses. *International Journal of Solids and Structures*, 23(1):111–131, 1987.
- [31] Toledano, A. and Murakami, H. A composite plate theory for arbitrary laminate configurations. *Journal of Applied Mechanics*, 54(1):181–189, 1987.
- [32] Carrera, E. Theories and finite elements for multilayered plates and shells: A unified compact formulation with numerical assessment and benchmarking. *Arch. Comput. Meth. Engng*, 10(3):215–296, 2003.
- [33] Carrera, E. *Finite Element Analysis of Structures through Unified Formulation*. John Wiley & Sons, 2014.
- [34] Carrera, E. and Antona, E. A class of two-dimensional theories for anisotropic multilayered plates analysis. *Memorie della Accademia delle scienze di Torino*, 19–20:49–97, 1995.
- [35] Carrera, E. C_z^0 requirements-models for the two dimensional analysis of multilayered structures. *Composite Structures*, 37(3–4):373–383, 1997. [http://dx.doi.org/10.1016/S0263-8223\(98\)80005-6](http://dx.doi.org/10.1016/S0263-8223(98)80005-6).

- [36] Carrera, E. Evaluation of layer-wise mixed theories for laminated plates analysis. *AIAA Journal*, 36(5):830–839, 1998. <http://dx.doi.org/10.2514/2.444>.
- [37] Carrera, E. Layer-wise mixed models for accurate vibration analysis of multilayered plates. *Journal of Applied Mechanics*, 65(4):820–828, 1998. <http://dx.doi.org/10.1115/1.2791917>.
- [38] Carrera, E. Transverse normal stress effects in multilayered plates. *Journal of Applied Mechanics*, 66:1004–1012, 1999. <http://dx.doi.org/10.1115/1.2791769>.
- [39] Carrera, E. A study of transverse normal stress effects on vibration of multilayered plates and shells. *Journal of Sound and Vibrations*, 225(5):803–829, 1999. <http://dx.doi.org/10.1006/jsvi.1999.2271>.
- [40] Carrera, E. Single- vs Multilayer Plate Modelings on the Basis of Reissner’s Mixed Theorem. *AIAA Journal*, 38(2):342–352, 2000. <http://dx.doi.org/10.2514/2.962>.
- [41] Carrera, E. A priori vs a posteriori evaluation of transverse stresses in multilayered orthotropic plates. *Composite Structures*, 48(4):245–260, 2000. [http://dx.doi.org/10.1016/S0263-8223\(99\)00112-9](http://dx.doi.org/10.1016/S0263-8223(99)00112-9).
- [42] Carrera, E. and Demasi, L. Classical and advanced multilayered plate elements based upon PVD and RMVT. Part 1: Derivation of finite element matrices. *International Journal for Numerical Methods in Engineering*, 55(2):191–231, 2002. <http://dx.doi.org/10.1002/nme.492>.
- [43] Carrera, E. and Demasi, L. Classical and advanced multilayered plate elements based upon PVD and RMVT. Part 2: Numerical implementations. *International Journal for Numerical Methods in Engineering*, 55(3):253–291, 2002. <http://dx.doi.org/10.1002/nme.493>.
- [44] Carrera, E. and Petrolo, M. On the Effectiveness of Higher-Order Terms in Refined Beam Theories. *Journal of Applied Mechanics*, 78:1–17, 2011.

- [45] Carrera, E. and Miglioretti, F. and Petrolo, M. Computations and evaluations of higher-order theories for free vibration analysis of beams. *Journal of Sound and Vibration*, 331:4269–4284, 2012.
- [46] Carrera, E. and Petrolo, M. Guidelines and recommendation to construct theories for metallic and composite plates. *AIAA Journal*, 48(12):2852–2866, 2010. doi: 10.2514/1.J050316.
- [47] Carrera, E. and Miglioretti, F. and Petrolo, M. Accuracy of refined finite elements for laminated plate analysis. *Composite Structures*, 93:1311–1327, 2011.
- [48] Carrera, E. and Miglioretti, F. and Petrolo, M. Guidelines and recommendations on the use of higher order finite elements for bending analysis of plates. *International Journal for Computational Methods in Engineering Science and Mechanics*, 12(6):303–324, 2011. doi:10.1080/15502287.2011.615792.
- [49] Carrera, E. and Miglioretti, F. Selection of appropriate multilayered plate theories by using a genetic like algorithm. *Composite Structures*, 94(3):1175–1186, 2012. doi: <http://dx.doi.org/10.1016/j.compstruct.2011.10.013>.
- [50] Petrolo, M. and Lamberti, A. and Miglioretti, F. Best Theory Diagram for Metallic and Laminated Composite Plates. *Mechanics of Advanced Materials and Structures*, In Press.
- [51] Mashat, D. S. and Carrera, E. and Zenkour, A. M. and Al Khateeb, S. A. Use of axiomatic/asymptotic approach to evaluate various refined theories for sandwich shells. *Composite Structures*, 109:139–149, 2014. doi: <http://dx.doi.org/10.1016/j.compstruct.2013.10.046>.
- [52] Mashat, D. S. and Carrera, E. and Zenkour, A. M. and Al Khateeb, S. A. Axiomatic/asymptotic evaluation of multilayered plate theories by using single and

- multi-points error criteria. *Composite Structures*, 106(0):393–406, 2013. doi: <http://dx.doi.org/10.1016/j.compstruct.2013.05.047>.
- [53] Petrolo, M. and Lamberti, A. Asymptotic/axiomatic analysis of refined layer-wise theories for composite and sandwich plates. *Mechanics of Advanced Materials and Structures*, In Press. doi: <http://dx.doi.org/10.1080/15376494.2014.924607>.
- [54] Carrera, E. and Cinefra, M. and Lamberti, A. and Petrolo, M. Results on best theories for metallic and laminated shells including Layer-Wise models. *Composite Structures*, In Press.
- [55] K.J. Bathe. *Finite element procedure*. Prentice hall, Upper Saddle River, New Jersey, 1996.
- [56] E. Carrera, G. Giunta, and M. Petrolo. *Beam Structures: Classical and Advanced Theories*. John Wiley & Sons, 2011.
- [57] Pagano, N. J. "Exact solutions for rectangular bidirectional composites and sandwich plate" *Journal of Composites Material* , 4:20–34, 1969.

Tables

	LM4									EM4								
u_x	■	▲	▲	▲	■	▲	▲	▲	■			▲	▲	▲	▲	▲		
u_y	■	▲	▲	▲	■	▲	▲	▲	■			▲	▲	▲	▲	▲		
u_z	■	▲	▲	▲	■	▲	▲	▲	■			▲	▲	▲	▲	▲		
σ_{xz}	■	▲	▲	▲	■	▲	▲	▲	■	■	▲	▲	▲	■	▲	▲	▲	■
σ_{yz}	■	▲	▲	▲	■	▲	▲	▲	■	■	▲	▲	▲	■	▲	▲	▲	■
σ_{zz}	■	▲	▲	▲	■	▲	▲	▲	■	■	▲	▲	▲	■	▲	▲	▲	■

Table 1: Full model representation of a two-layer model in the case of an LM4 description of displacements and transverse stresses, and in the case of an ED4 description of displacements and LD4 for transverse stresses (EM4).

Active term	Inactive term	Non-deactivable term
▲	△	■

Table 2: Symbols to indicate the status of a displacement variable.

■	▲	△	▲	■	▲	▲	▲	■
■	▲	▲	▲	■	▲	▲	▲	■
■	▲	▲	△	■	▲	▲	▲	■
■	▲	▲	▲	■	▲	▲	▲	■
■	▲	▲	▲	■	△	▲	▲	■
■	▲	▲	▲	■	▲	▲	△	■

Table 3: Representation of the reduced model.

	$\bar{\sigma}_{xx}(z = \pm h/2)$		$\bar{\sigma}_{xz}(z = 0)$	$\bar{\sigma}_{yz}(z = 0)$	$\bar{u}(z =, h/2)$
	$a/h = 100$				
Pagano [57]	± 0.539		0.395	0.0828	N/A
LM4	± 0.539		0.395	0.0828	0.4347
LD4	± 0.539		0.395	0.0828	0.4347
EM4	± 0.539		0.301	0.0706	0.4343
ED4	± 0.539		0.281	0.0734	0.4342
	$a/h = 4$				
Pagano [57]	0.801	-0.755	0.256	0.2172	N/A
LM4	0.801	-0.755	0.256	0.2172	2.1216
LD4	0.801	-0.755	0.256	0.2180	2.1216
EM4	0.791	-0.745	0.219	0.1767	2.0271
ED4	0.786	-0.740	0.205	0.1830	2.0083

Table 4: Stress and displacement values for a $0^\circ/90^\circ/0^\circ$ simply-supported laminated plate.

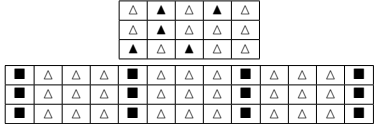

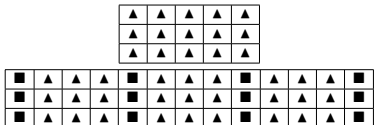

	EM4	ED4
	$a/h = 100$	
M_e/M	17/54	5/15
		
Error	0.0148%	0.0148%
	$a/h = 4$	
M_e/M	54/54	15/15
		
Error	1.1941%	1.7951%

Table 5: Reduced EM4 and ED4 models for the symmetric laminated plate, σ_{xx}



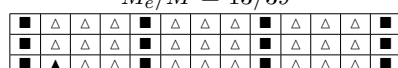

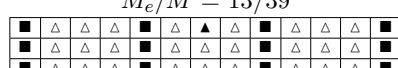
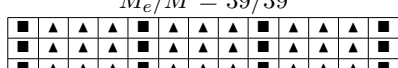
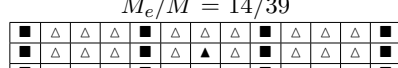
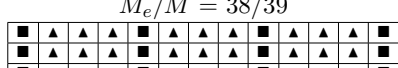
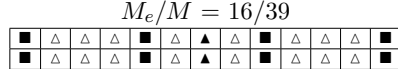
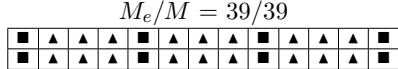
	$a/h = 100$	$a/h = 4$
	$M_e/M = 12/39$	$M_e/M = 20/39$
u_z		
	$M_e/M = 13/39$	$M_e/M = 21/39$
σ_{xx}		
	$M_e/M = 13/39$	$M_e/M = 39/39$
σ_{xz}		
	$M_e/M = 14/39$	$M_e/M = 38/39$
σ_{yz}		
	$M_e/M = 16/39$	$M_e/M = 39/39$
COMBINED		

Table 6: Reduced LD4 models for the symmetric laminated plate.

	$a/h = 100$ $M_e/M = 24/78$	$a/h = 4$ $M_e/M = 37/78$
u_z		
σ_{xx}	$M_e/M = 26/78$ 	$M_e/M = 42/78$
σ_{xz}	$M_e/M = 35/78$ 	$M_e/M = 46/78$
σ_{yz}	$M_e/M = 36/78$ 	$M_e/M = 45/78$
COMBINED	$M_e/M = 45/78$ 	$M_e/M = 56/78$

Table 7: Reduced LM4 models for the symmetric laminated plate.

	$\bar{\sigma}_{xx}(z = \pm h/2)$		$\bar{\sigma}_{xz}(z = 0)$	$\bar{\sigma}_{yz}(z = 0)$	$\bar{u}_z(z = h/2)$
	$a/h = 100$				
LM4	0.0844	-0.7159	0.1221	0.1221	1.0652
LD4	0.0844	-0.7159	0.1221	0.1221	1.0652
EM4	0.0843	-0.7158	0.1631	0.1631	1.0651
ED4	0.0842	-0.7157	0.2800	0.1120	1.0651
	$a/h = 4$				
LM4	0.1098	-0.7897	0.1379	0.1230	2.1700
LD4	0.1098	-0.7896	0.1439	0.1205	2.1700
EM4	0.1094	-0.7748	0.1672	0.1585	2.1385
ED4	0.1093	-0.7708	0.2878	0.1091	2.1282

Table 8: Stress and displacement values for a $0^\circ/90^\circ$ simply-supported laminated plate.

	EM4	ED4
	$a/h = 100$	
M_e/M	16/42	7/15
Error	0.0141%	0.0265%
	$a/h = 4$	
M_e/M	42/42	15/15
Error	1.4533%	1.9272%

Table 9: Reduced EM4 and ED4 models for asymmetric laminated plate, u_z

	$a/h = 100$	$a/h = 4$
	$M_e/M = 11/27$	$M_e/M = 16/27$
u_z		
	$M_e/M = 11/27$	$M_e/M = 19/27$
σ_{xx}		
	$M_e/M = 13/27$	$M_e/M = 27/27$
σ_{xz}		
	$M_e/M = 13/27$	$M_e/M = 27/27$
σ_{yz}		
	$M_e/M = 15/27$	$M_e/M = 27/27$
COMBINED		

Table 10: Reduced LD4 models for the asymmetric laminated plate.

	$a/h = 100$ $M_e/M = 20/54$	$a/h = 4$ $M_e/M = 28/54$
u_z		
	$M_e/M = 20/54$	$M_e/M = 43/54$
σ_{xx}		
	$M_e/M = 28/54$	$M_e/M = 38/54$
σ_{xz}		
	$M_e/M = 28/54$	$M_e/M = 40/54$
σ_{yz}		
	$M_e/M = 34/54$	$M_e/M = 52/54$
COMBINED		

Table 11: Reduced LM4 models for the asymmetric laminated plate.

	$\bar{\sigma}_{xx}(z = \pm h/2)$		$\bar{\sigma}_{xz}(z = 0)$	$\bar{\sigma}_{yz}(z = 0)$	$\bar{u}_z(z = h/2)$
	$a/h = 100$				
LM4	0.2236	-0.1810	0.2355	0.2355	2.2073
LD4	0.2236	-0.1810	0.2355	0.2355	2.2073
EM4	0.2244	-0.1803	0.2316	0.2316	2.2072
ED4	0.2246	-0.1804	0.1846	0.1845	2.2072
	$a/h = 4$				
LM4	0.2520	-0.1830	0.2306	0.2307	2.9079
LD4	0.2520	-0.1830	0.2306	0.2306	2.9079
EM4	0.2514	-0.1840	0.2287	0.2286	2.8982
ED4	0.2521	-0.1845	0.1823	0.1822	2.8945

Table 12: Stress and displacement values for a bimetallic simply-supported laminated plate.

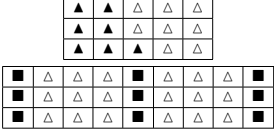

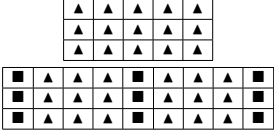
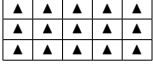
	EM4	ED4
	$a/h = 100$	
M_e/M	16/42	7/15
		
Error	0.0406%	0.0458%
	$a/h = 4$	
M_e/M	42/42	15/15
		
Error	0.3305%	0.4596%

Table 13: Reduced EM4 and ED4 models for the bimetallic plate, u_z











	$a/h = 100$	$a/h = 4$
	$M_e/M = 11/27$	$M_e/M = 17/27$
u_z		
	$M_e/M = 11/27$	$M_e/M = 19/27$
σ_{xx}		
	$M_e/M = 13/27$	$M_e/M = 20/27$
σ_{xz}		
	$M_e/M = 13/27$	$M_e/M = 20/27$
σ_{yz}		
	$M_e/M = 15/27$	$M_e/M = 24/27$
COMBINED		

Table 14: Reduced LD4 models for the bimetallic plate.

	$a/h = 100$ $M_e/M = 20/54$	$a/h = 4$ $M_e/M = 30/54$
u_z		
σ_{xx}	$M_e/M = 20/54$ 	$M_e/M = 40/54$
σ_{xz}	$M_e/M = 28/54$ 	$M_e/M = 40/54$
σ_{yz}	$M_e/M = 28/54$ 	$M_e/M = 41/54$
COMBINED	$M_e/M = 34/54$ 	$M_e/M = 50/54$

Table 15: Reduced LM4 models for the bimetallic plate.

Figures

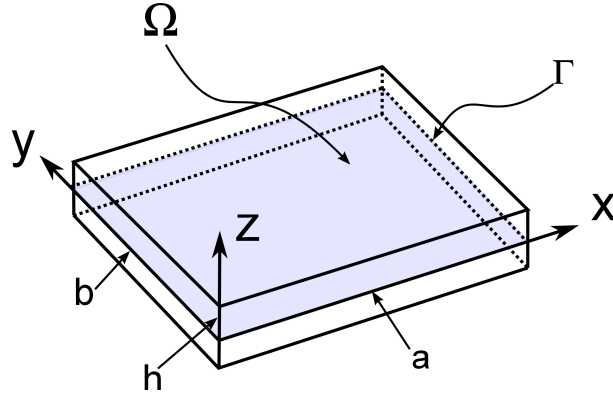


Figure 1: Plate geometry and reference frame.

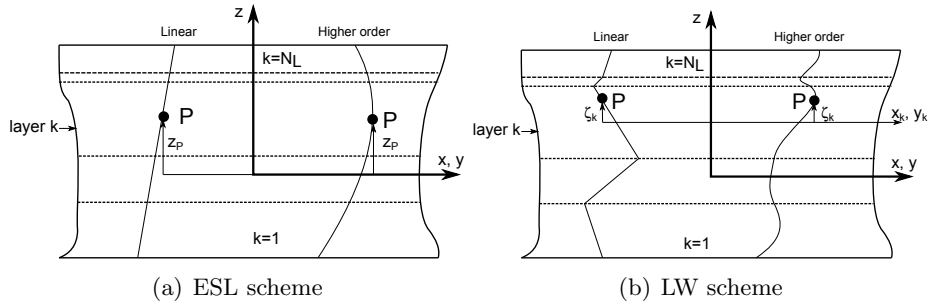


Figure 2: Equivalent Single Layer (ESL) scheme and Layer Wise (LW) scheme.

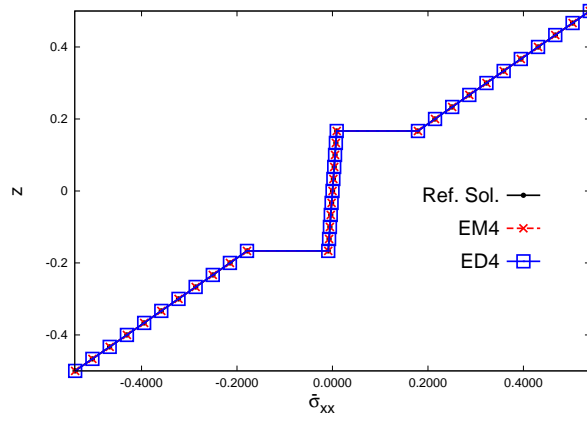
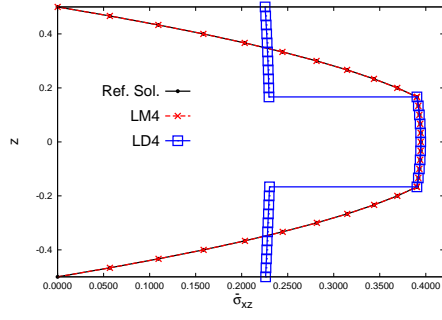
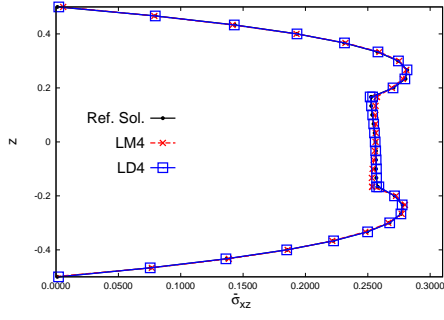


Figure 3: σ_{xx} distribution along the thickness via an EM4 model, symmetric laminated plate, $a/h = 100$.

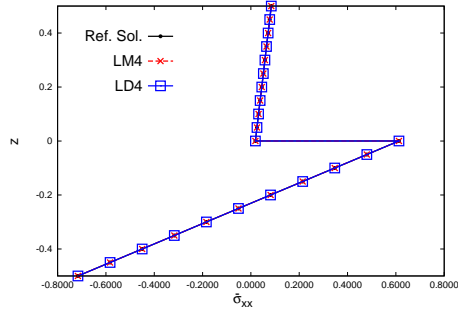


(a) $a/h = 100$

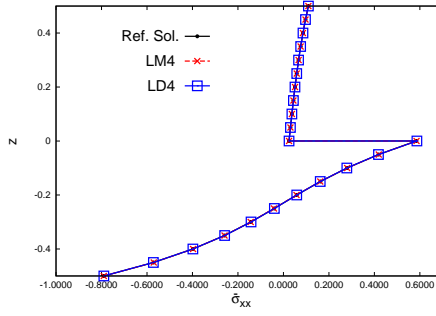


(b) $a/h = 4$

Figure 4: σ_{xz} distribution along the thickness via LD4 and LM4 reduced models, symmetric laminated plate.

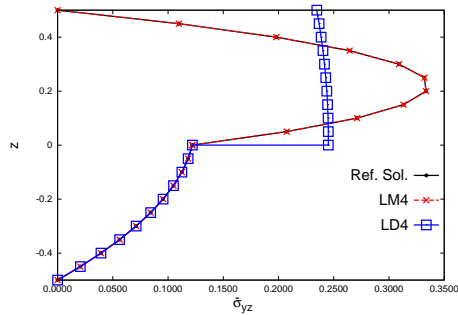


(a) $a/h = 100$

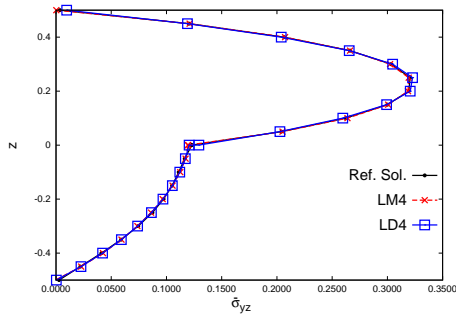


(b) $a/h = 4$

Figure 5: σ_{xx} distribution along the thickness via LD4 and LM4 reduced models, asymmetric laminated plate.



(a) $a/h = 100$



(b) $a/h = 4$

Figure 6: σ_{yz} distribution along the thickness via LD4 and LM4 reduced models, asymmetric laminated plate..

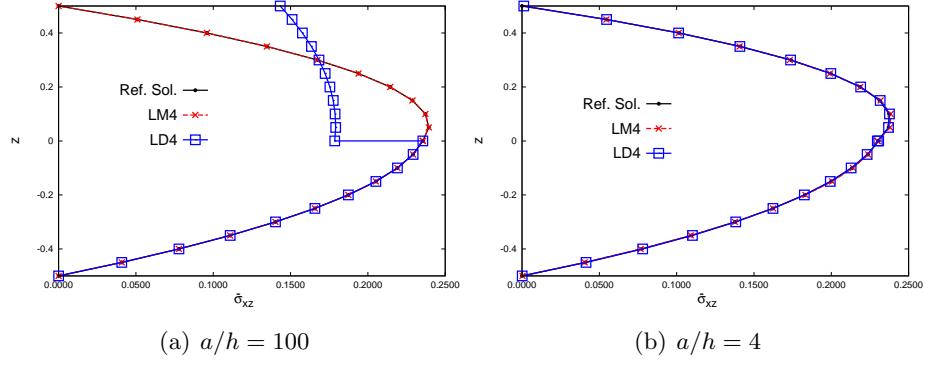


Figure 7: σ_{xz} distribution along the thickness via LD4 and LM4 reduced models, bimetallic plate.